

Evaluation of interphase properties in a cellulose fiber-reinforced polypropylene composite by nanoindentation and finite element analysis

Seung-Hwan Lee ^{a,*}, Siquan Wang ^a, George M. Pharr ^{b,c}, Haitao Xu ^b

^a Tennessee Forest Products Center, University of Tennessee, Knoxville, TN, United States

^b Department of Material Science, University of Tennessee, Knoxville, TN, United States

^c Metals and Ceramic Division, Oak Ridge National Laboratory, Oak Ridge, TN, United States

Received 26 June 2006; received in revised form 20 November 2006; accepted 7 January 2007

Abstract

The hardness and elastic modulus of the cellulose fiber and polypropylene (PP) matrix in a cellulose fiber-reinforced PP composite were investigated by nanoindentation with a continuous stiffness technique. Nanoindentation with different indentation depths and spacings was conducted to measure hardness and elastic modulus in the interphase region, which was modified by maleic anhydride-grafted PP and γ -amino propyltrimethoxy silane (γ -APS) sizing. A line of indents was produced from the fiber to the matrix. There was a gradient of hardness and modulus across the interphase region. The distinct properties of the transition zone were revealed by 1–4 indents, depending on nanoindentation depth and spacing. Based on the results of nanoindentation, it was assumed that the width of the property transition zone is less than 1 μm . However, three dimensional finite element analysis shows that even a perfect interface without property transition has almost same interphase width as that measured by nanoindentation. Using existing nanoindentation techniques, it will be difficult to calculate exact mechanical properties without the effect of neighboring material property in at least 8 times smaller region than indent size. © 2007 Elsevier Ltd. All rights reserved.

Keywords: A. Natural fibre composites; B. Hardness; B. Interface/interphase; C. Finite element analysis (FEA)

1. Introduction

Researchers studying composites are considering natural fibers for composite materials, suggesting these are a viable alternative to conventional fibers such as glass, carbon or aramid fibers and talc [1–4]. Natural fibers have numerous advantages, for example; low cost, low density, high toughness, acceptable specific strength properties, ease of processing and separation, and biodegradability. Furthermore, the use of natural resources reduces releases of carbon dioxide and can aid in the conservation of petroleum.

Natural fiber-reinforced polymer composites (NFRPC) have also attracted attention as a method of recycling

natural fibers and plastic waste, and for preparing water-resistant natural fiber-based materials without using formaldehyde-based adhesives [5–10]. The greatest growth potential for NFRPCs is in the building industries. Products known commonly as “wood-plastic composites” include decking, fencing, industrial flooring, landscape timber, railings, and molding [11]. In particular, the decking market is the largest and fastest growing NFRPC market.

In fiber-reinforced polymer composites, it is widely accepted that the performance of a composite as a structural material depends mainly on the quality of the stress transfer in the interphase. The interphase in fiber-reinforced composite is a transition region, which extends nanometers to microns over which the mechanical and physical properties change from the bulk properties of fiber to the bulk properties of the polymer. This interphase has a heterogeneous nature, with different morphological features,

* Corresponding author. Tel.: +1 865 974 4965; fax: +1 865 946 1109.
E-mail address: lshyhk@hotmail.com (S.-H. Lee).

chemical compositions and mechanical properties from those of the reinforcing fiber or the matrix polymer [12,13]. It is conceivable that the nature of the interphase would vary with the specific composite system.

An appropriately engineered interphase can significantly improve the strength and toughness of composites as well as the environmental stability [14]. For example, an interphase that is softer than the surrounding polymer would result in lower overall stiffness and strength, but greater resistance to fracture [12,15,16]. On the other hand, an interphase that is stiffer than the surrounding polymer would give the composite less fracture resistance but make it very strong and stiff [17]. Therefore, a better understanding of interfacial properties and characteristics will be helpful in evaluating the overall properties of fiber-reinforced polymer composite materials and will enable optimal design of composite materials [18,19].

However, the nature of the interphase within a thickness less than 5 μm is rarely reported in the literature because experimental means of unequivocally establishing the interphase properties are lacking. Nanoindentation testing is a new approach to measure the size and relative mechanical properties of interphases. This technique can determine the mechanical properties of a material on the nanoscale [20–25]. The nanoindentation technique utilizes the same principle as microindentation or micro-hardness testing. The difference is that in nanoindentation the probe and loads are much smaller, so as to produce indentations a few micrometers to a few hundred nanometers in size.

Very few studies have been performed on nanoindentation measurement of the interphase in fiber-reinforced polymer composites system, such as glass or carbon fiber-reinforced thermally-cured resin composite system and thermoplastic matrix composite system [19,24]. This technique has not yet been applied to the interfacial properties in natural fiber-reinforced composites, even though the evaluation of the interfacial properties in these composites is also important.

This study investigated the mechanical properties in the interphase in cellulose fiber-reinforced PP composites using nanoindentation with a continuous stiffness measurement (CSM) technique. The CSM technique is a significant improvement in nanoindentation testing. It offers a direct measure of dynamic contact stiffness during the loading portion of an indentation test and, being somewhat insensitive to thermal drift, allows an accurate observation of small volume deformation [23].

2. Experimental

2.1. Materials

Lyocell fiber (1.7 decitex) with around 12 μm diameter and 38 mm length was supplied by Tencel Inc., NY. Isotactic polypropylene ($M_w = 16 \times 10^4$) was provided by Fiber Visions, Inc. (Covington, GA) in the form of fiber bundles. For chemical modification, maleic anhydride-grafted PP

(EPOLENE G-3003), with an acid number of 8 and an average molecular weight (M_w) of 52,000, and γ -amino propyltrimethoxy silane (γ -APS) were purchased from Eastman Chemicals and Sigma Aldrich, respectively. Other chemicals were purchased from commercial sources.

2.2. Silane treatment of lyocell fiber

A solution of γ -APS was prepared by adding 3 g of silane to 150 ml of a methanol-water mixture (9/1 volume ratio) and stirred for 15 min. A 10 g of lyocell fiber was added to the silane solution and kept for 60 min. The silane coated fibers were rinsed with pure water and dried and cured in an oven at 60 $^\circ\text{C}$.

2.3. Preparation of specimens

PP and MAPP (10% wt% based on PP weight) were first mixed in dry solid states followed by blending using a Labo Plastomill (Toyo Seiki). The temperature, rotation rate, and processing time were 200 $^\circ\text{C}$, 50 rpm, and 10 min, respectively. The obtained product was compression-molded into a film with a thickness of 0.4 mm. Silane-treated lyocell fiber was unidirectionally placed on PP-MAPP film and the films were stacked and compression-molded at 200 $^\circ\text{C}$ for 10 min to obtain the unidirectional lyocell fiber-reinforced PP composites.

The composite was cut into a small block and was glued to an acrylic block. The acrylic block was then mounted onto an ultramicrotome and the specimen was cross-sectionally cut with a glass knife. Finally, the surface was smoothed using a diamond knife. The smoothed specimens were conditioned for at least 24 h at 21 $^\circ\text{C}$ and 60% relative humidity in a room that housed the nanoindenter and AFM.

2.4. Atomic force microscopy (AFM)

The topography of the sample was taken by AFM APHB-0100 (Park Scientific Instruments) operated in contact mode. The surface of specimen had a vertical range of 100–250 nm with a root mean square (rms) surface roughness amplitude of 20–30 nm and an average roughness of 15–20 nm. Fig. 1 shows the AFM height image. The fiber appears on the left-hand side of the image. Two indentations with 100 nm depth can be seen in the PP matrix (right-hand side).

2.5. Nanoindentation (continuous stiffness measurement)

A continuous stiffness measurement that involved a progressive series of loading and partial unloading cycles was conducted until the final indentation depth was achieved, generating series of hardness and modulus values as a function of indentation depth. Three different final indentation depths, 30, 50, and 100 nm, were used with spacings between adjacent indents of 260, 400, 800, and 1600 nm respectively to avoid overlapping of plastic deformation

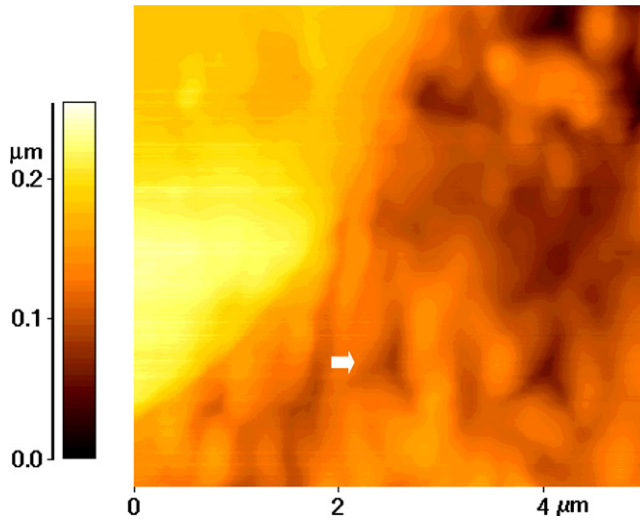


Fig. 1. AFM height image of the surface of the specimen.

zones onto neighboring indents. Continuous nanoindentation was performed following six steps: a careful approach to the surface, loading to peak load, holding the indenter at peak load, unloading 90% of peak load for 50 s, holding the indenter after 90% unloading for 100 s, and finally, unloading completely. An arrayed line of indents was made from fiber and matrix with different spacing, depending on indentation depth.

Hardness (H) and elastic modulus (E) were calculated from the load–displacement data. As the indenter penetrates into the sample, both elastic and plastic deformation occurs and only the elastic portion of the displacement is recovered during unloading. Nanoindentation hardness is defined as:

$$H = \frac{P_{\max}}{A}, \quad (1)$$

where P_{\max} is the load measured at a maximum depth of penetration (h) in an indentation cycle; A is the projected contact area ($24.5 h_c^2$); and h_c is the contact depth of indent.

The elastic modulus of the sample can be inferred from the initial unloading contact stiffness (S), i.e., the slope ($\frac{dP}{dh}$) of the initial portion of the unloading curve. A relation among contact stiffness, contact area, and elastic modulus can be derived as:

$$S = 2\beta\sqrt{\frac{A}{\pi}}E_r, \quad (2)$$

where β is a constant that depends on the geometry of the indenter ($\beta = 1.034$ for a Berkovich indenter) and E_r is reduced elastic modulus, which accounts for the fact that elastic deformation occurs in both the sample and the indenter.

The sample elastic modulus (E_s) can then be calculated as [25]:

$$E_s = (1 - \nu_s^2) \left(\frac{1}{E_r} - \frac{1 - \nu_i^2}{E_i} \right)^{-1}, \quad (3)$$

where ν_s and ν_i (0.07) are the Poisson's ratios of the specimen and indenter, respectively, while E_i is the modulus of the indenter (1141 GPa).

3. Results and discussion

3.1. Evaluation of hardness and elastic modulus for pure matrix and fiber

Fig. 2 shows a series of hardness (H) and elastic modulus (E) values of cellulose fiber and PP matrix obtained by continuous nanoindentation with 100 nm depth. It was found that these values became constant after an indentation depth of 30 nm. The variation in region below 30 nm indentation depth may be due to the roughness of the sample, which was 20–30 nm (rms surface roughness). This indicates that the 100 nm indentation depth used in this study to evaluate interphase properties is deep enough to

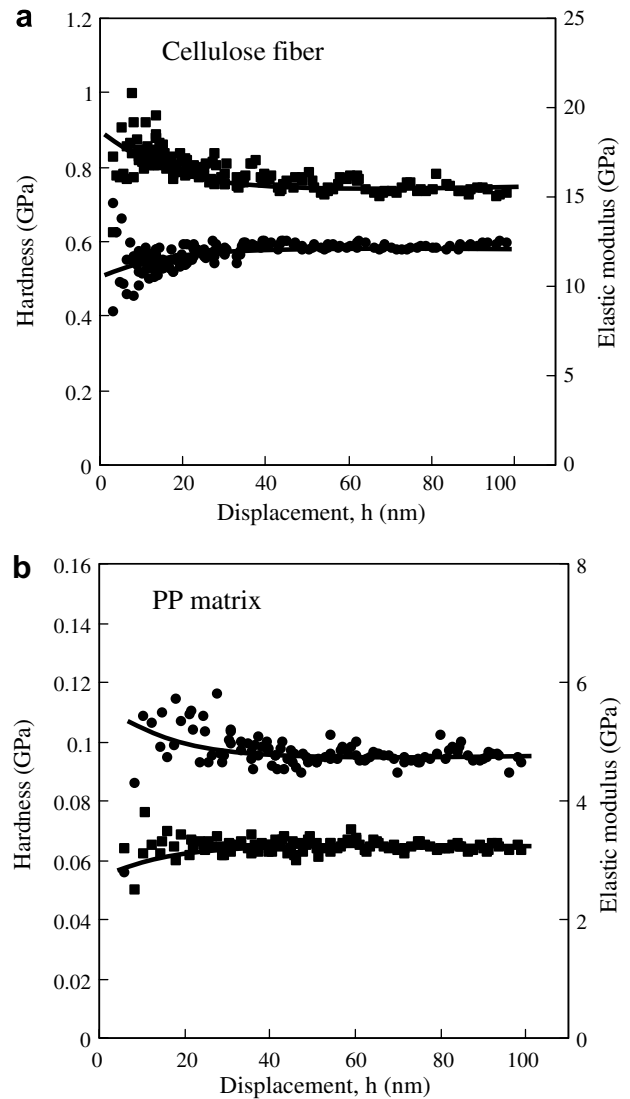


Fig. 2. The dependency of hardness (●) and elastic modulus (■) on indentation depth.

Table 1
Two expressions of hardness and elastic modulus obtained by continuous nanoindentation

Sample	Mean value from 50 to 100 nm depth, GPa		Unloading value at final indentation depth, GPa	
	H_{mean}	E_{mean}	H_{u}	E_{u}
Lyocell fiber	0.62 (0.01)	16.62 (0.13)	0.62 (0.01)	16.10 (0.30)
PP/MAPP Matrix	0.11 (0.01)	3.03 (0.17)	0.12 (0.02)	3.08 (0.06)

Each is the average value from 5 indents. The value in parenthesis is the standard deviation (SD).

reach constant elastic modulus and hardness, irrespective of our sample surface roughness.

The hardness and elastic moduli of the samples were expressed as two different values. The first was a mean value from 50 to 100 nm indentation depth. The other was the value from an unloading at final indentation depth. These values were obtained by averaging 5 indents in different locations, and are summarized in Table 1. There was no significant difference between the values for mean value from 50 to 100 nm depth and for unloading value at final indentation depth (two-sample T-test, $\alpha = 0.05$). Tze et al. have recently conducted continuous nanoindentation to evaluate the nano-scale hardness and elastic modulus of wood cell walls [26]. They have reported that the hardness and elastic modulus of natural wood fibers were 0.41–0.54 GPa and 12.7–19.3 GPa, respectively, depending on cellulose microfibril angle. Gindl et al. [27] reported that the hardness and elastic modulus of lyocell fiber were 0.3–0.7 GPa and 11–17 GPa, respectively, depending on the nanoindentation depth [27]. These values are very similar to those of this study but half of the 36 GPa reported for the microscopic tensile modulus of lyocell fibers with an average diameter of 10–12 μm [28].

Gao et al. reported the mean elastic modulus of a PP matrix of 1.85 GPa, which was obtained by single-step nanoindentation with a contact depth of 7.1 nm and indentation force of 0.24 μN [21]. This value is somewhat lower than our result obtained by continuous nanoindentation. However, it is natural that there is a wide variation of mechanical properties of PP with different molecular weight, crystallinity, etc. The PP/MAPP matrix in this study showed a crystallinity of 36.7% based on DSC measurements. The effect of crystallization on nanoscale properties in natural fiber-reinforced composites is the focus of an upcoming publication. The values obtained in this study are comparable to the reported values from a macroscopic tensile test [29]. The values of elastic modulus and hardness from the final unloading were used in following discussion.

3.2. Evaluation of the size and mechanical properties of the interphase

Fig. 3 illustrates the profiles of hardness and elastic modulus across the interphase region between the fiber and PP matrix, which were obtained from an unloading at the final indentation depth (100 nm). The spacing of indents was

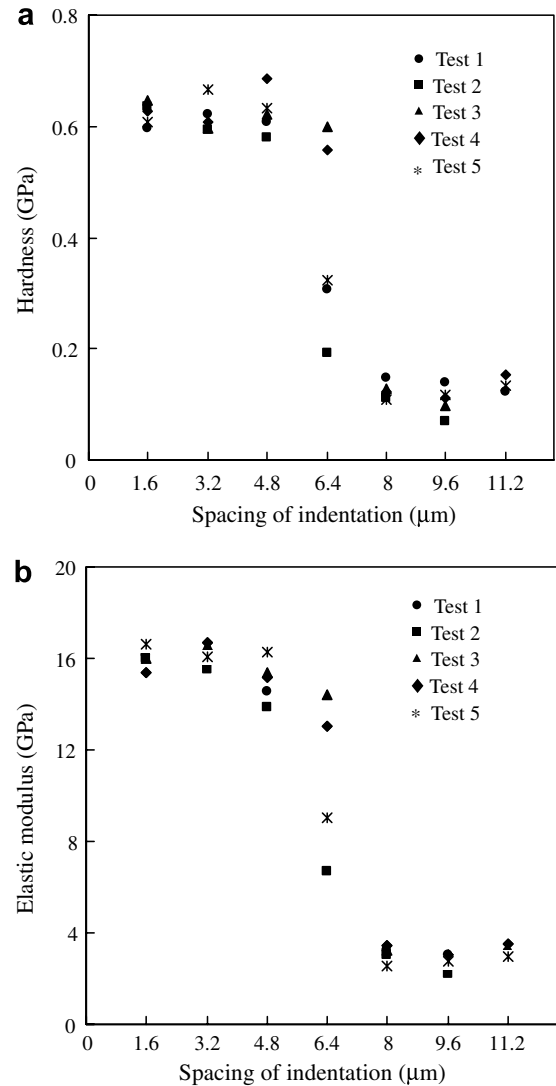


Fig. 3. Variation of hardness (a) and elastic modulus (b) across the interphase region between the fiber and PP matrix obtained by nanoindentation with 50 nm depth and 1600 nm spacing.

1.6 μm to avoid overlapping the plastic zone of neighboring indents. When the indenter is pressed into the materials, it creates a corresponding stress field, i.e., the zone associated with plastic deformation. Hodzic et al. have reported that this zone is approximately equal to twice the maximum width of the nanoindentation [22]. Based on the geometry of Berkovich indenter used in this study, the width of indentation can be calculated by following equation:

$$s = 2h(\tan 65.3^\circ)/(\tan 30^\circ), \quad (4)$$

where s is the width of indentation and h is indentation depth. As h is 100 nm, the width of indentation is 753 nm. Thus the spacing of 1.6 μm is long enough to avoid the effect of a stress field from plastic deformation.

Two of the five experiments resulted in one indent with distinct hardness and elastic modulus in transition zone, showing intermediate properties between those for fiber and matrix (Fig. 3). The transition zone can be regarded

as the interphase. However, it is difficult to estimate the effective interphase width by only one indent with a large size (756 nm width), considering the increasing resistance to indentation in locations close to the fiber. If the indent is made in close proximity to the fiber, or touches the fiber edge during indentation, the resistance to indentation should be increased, because the development of a plastic zone by indentation will be constricted. In fact, one of the indents in the transition zone showed the linearly increasing trend with increasing indentation depth without leveling off to 100 nm depth as shown in Fig. 4. This means that the indenter tip was touching the fiber edge during indentation. To obtain the effective thickness of the interphase with reasonable accuracy, indentations should be made as small as possible.

Therefore, nanoindentations with 50 nm depth and 800 nm spacing were conducted and the results are summarized in Fig. 5. In these experiments, only one indent was also found in the transition zone, which can be inferred as less than 1600 nm. However, the nanoindentation with 800 nm spacing is still not sensitive enough to measure the effective thickness of the interphase. With the same indentation depth, the nanoindentations were performed by using 400 nm spacing instead of 800 nm. This spacing is not enough to avoid overlapping of the zone associated by plastic deformation, but the neighboring indent will not be overlapped. Even though it is difficult to obtain the quantitative value of properties, this trial is still meaningful to evaluate the interphase width and relative properties. Fig. 6 shows the variation of hardness and elastic modulus across the interphase region, indicating 2–3 indents in the transition zone per each experiment. It is notable that, among the indents made in transition zone, the properties of the indentations close to matrix should be affected less than those close to fiber. In other words, the results provided by these indents could not be merely influenced by the presence of the fiber. Furthermore, nano-

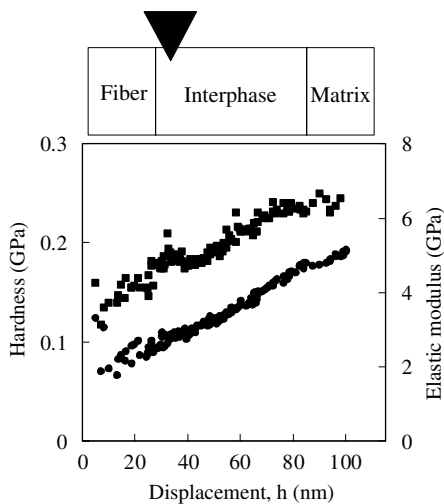


Fig. 4. An increase of hardness (●) and elastic modulus (■) with indentation depth in nanoindentation made in close proximity to the fiber.

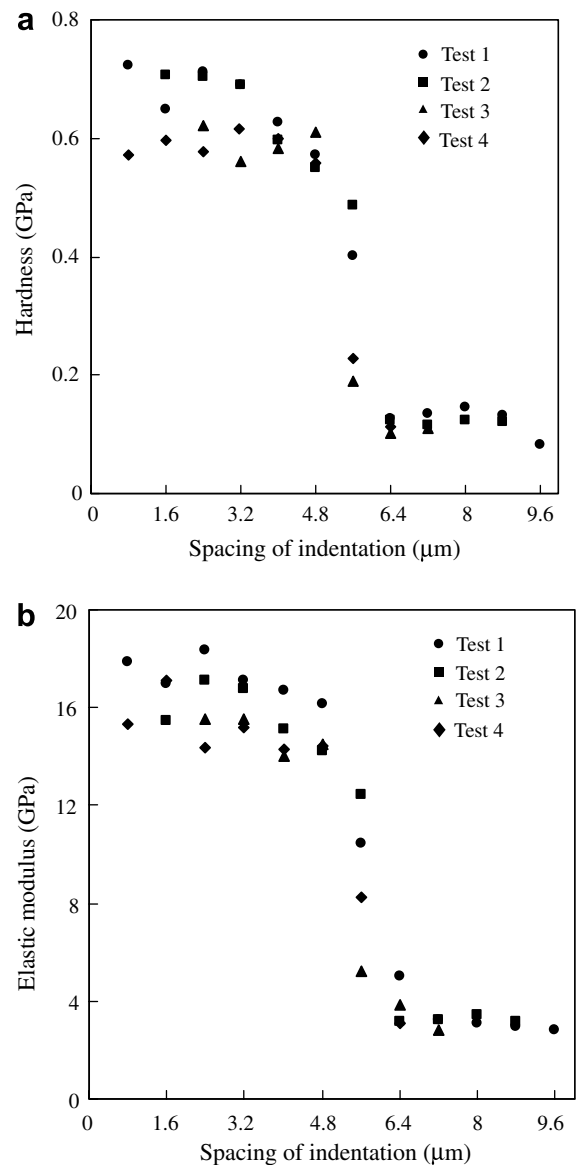


Fig. 5. Variation of hardness (a) and elastic modulus (b) across the interphase region between the fiber and PP matrix obtained by nanoindentation with 50 nm depth and 800 nm spacing.

indentation results (Fig. 7) obtained by using 30 nm depth and 260 nm spacing showed 4 indents with apparently distinct properties between fiber and matrix in the transition zone. Based on these nanoindentation results, it can be said that the width of interphase region is less than 1 μm.

It is conceivable that the nature of the interphase would vary with the specific composite system. It has been reported in phenolic resin or polyester resin/glass fiber composites that the single-step nanoindentation with indent depth as small as 30 nm showed distinct properties with 2–3 indents in transition zone [22]. The interphase thickness in vinyl ester/glass fiber composite has been reported as approximately 1 μm by single-step nanoindentation with 60 nm depth and 400 nm spacing [30]. This nanoindentation showed one or two indents in the transition zone, depending

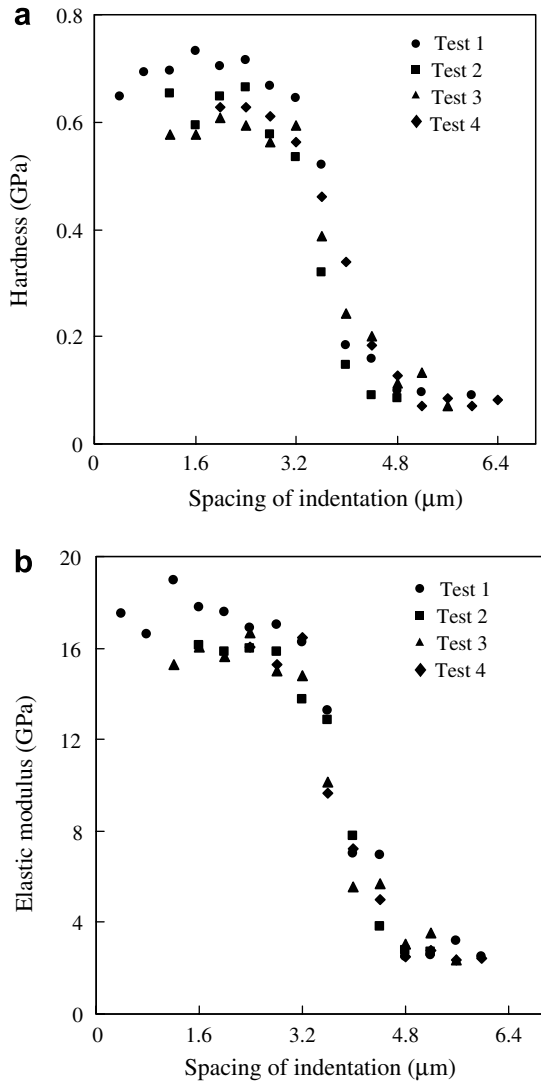


Fig. 6. Variation of hardness (a) and elastic modulus (b) across the interphase region between the fiber and PP matrix obtained by nanoindentation with 50 nm depth and 400 nm spacing.

on different silanes (γ -methacryl silane and γ -glycidoxypropyl-trimethoxysilane) and their concentration. In a glass fiber-reinforced epoxy composite system, when γ -aminopropyltriethoxy silane (γ -APS)/polyurethane sizing and γ -APS/PP sizing were used, the interphase thickness varied between less than 100 and \sim 300 nm, depending on the type of sizing by nanoindentations, with 1–10 nm depth (load range from 0.17–12 μ N) and 40 nm spacing [21].

3.3. Finite element analysis (FEA)

To support the results of nanoindentation above, three dimensional finite element analysis was conducted by using a rigid flat cylindrical punch with a radius of 1 μ m and the ABAQUS[®] finite element code. The finite element mesh and specimen geometry are shown in Fig. 8. Due to symmetry, only half of the specimen was modeled assuming a PP/MAPP matrix with elastic modulus of 4.67 GPa and a

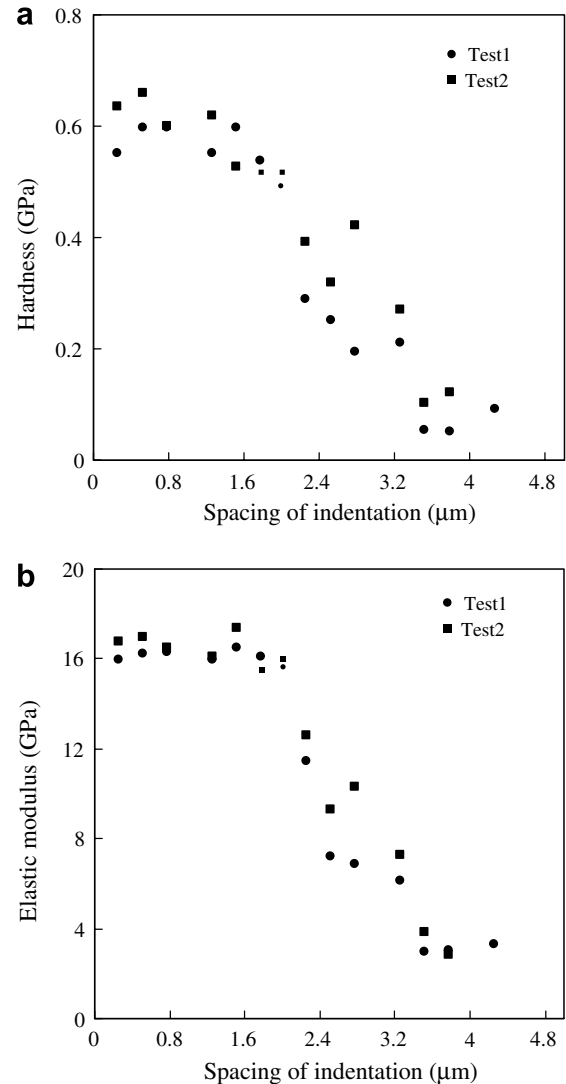


Fig. 7. Variation of hardness (a) and elastic modulus (b) across the interphase region between the fiber and PP matrix obtained by nanoindentation with 30 nm depth and 260 nm spacing.

cellulose fiber with an elastic modulus of 18.65 GPa. The Poisson ratio of both materials was assumed to be 0.3. The specimen, consisted of one cube each of the matrix and fiber materials 100 μ m on a side, was perfectly bonded at a single distinct interface. No friction was assumed, and the indentation depth was fixed at 50 nm.

Simulations by FEA were carried out to determine the stiffness at 17 different locations, the first being with the punch centered on the interface. The punch was then moved in both directions from the interface in 1 μ m increments for a total of 8 measurements in the fiber and 8 in the matrix. The adequacy of the mesh was tested by comparing simulation results for the homogeneous matrix and fiber materials with the known analytical solution given in Eq. (2). The FEA results differed from the exact solution by no more than 2%.

Fig. 9 shows the contact stiffness simulated by FEA as a function of distance from the perfect interface without

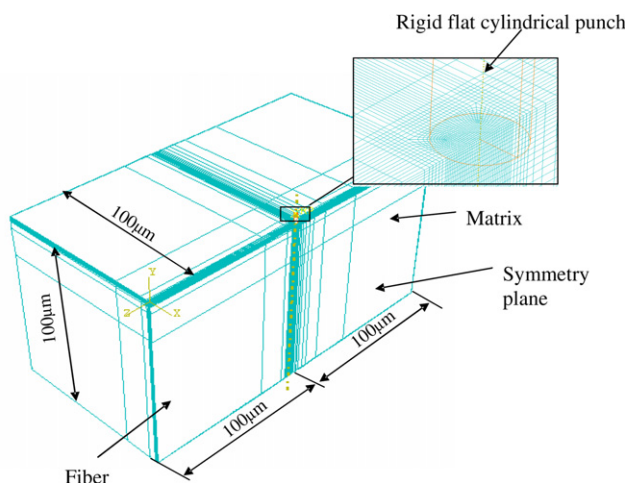


Fig. 8. Schematic illustration of the three dimensional finite element model and an enlarged view of the mesh in the region of contact.

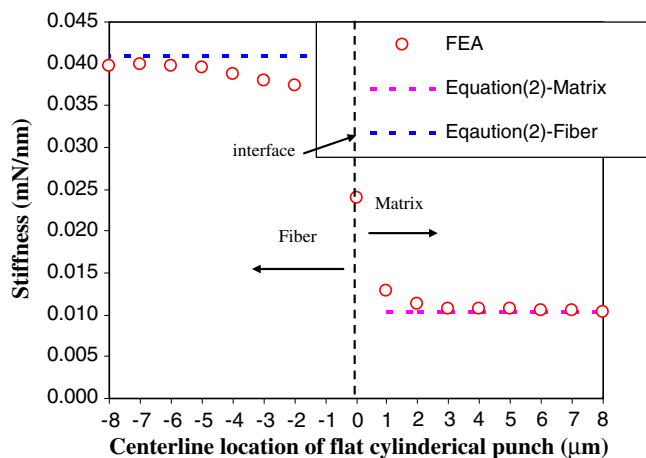


Fig. 9. Variation of the stiffness measured from the FEA with position from the interface. The punch radius is 1 μm .

property transition. Far from the interface, the stiffness of the fiber and matrix are approached, but within approximately 5 contact radii on the stiffer fiber side and 3 contact radii on the more compliant matrix side, the stiffness varies in a measurable way from that of the monolithic fiber or matrix. Thus, there is a transition zone approximately 8 contact radius wide in which the contact stiffness varies. However, it must be noted that this result is strictly based on a geometric effect, that is, it has nothing to do with real variations in material properties in the zone.

The width of the indent contact area in the nanoindentation using 30 nm depth and 260 nm spacing is around 224 nm. Assuming that this FEA analysis is applicable for nanoindentation using a Berkovich indenter, when the width of indent contact area is 224 nm, the perfect interface without property transition would be approximately 1.8 μm . That is, it would be difficult to say that the transition region estimated by nanoindentation shows

a distinct interphase region, without the effect of the neighboring material's property. Therefore, it must be concluded that it would be difficult to calculate the exact mechanical properties without including the effect of neighboring material properties in a region at least 8 times smaller than the indent size. However, a deconvolution approach to extract the real properties and dimensions of an interphase is potentially possible from the nanoindentation experimental results across the interphase, which could be fit to FEA results as a function of the properties and thickness of the interphase, even though it would be still difficult in practice unless the interphase was sufficiently thick and had sufficiently different properties than both the fiber and the matrix.

4. Conclusion

Two different approaches using nanoindentation with a continuous stiffness measurement were used to express the hardness and elastic modulus of cellulose fiber and PP matrix in the composite material. There was no significant difference among the mean value from 50 to 100 nm depth, the unloading value at final indentation depth. The mean values for hardness and elastic modulus values were 0.62 and 16.62 GPa in the cellulose fiber and 0.11 and 3.03 GPa in the PP matrix, respectively.

Nanoindentation was also conducted to measure hardness and elastic modulus in the interphase region, which is modified by maleic anhydride-grafted PP and γ -APS sizing. Even though the nanoindentation showed an approximately 1 μm wide property transition zone, the FEA-based results showed that the property transition in the interphase region is not completely due to the properties of a real interphase. Therefore, using existing nanoindentation techniques, it would be difficult to calculate the exact mechanical properties without considering the effect of neighboring material properties in an area at least 8 times smaller than the indent size. Our data suggests that nanoindents need to be made as small as possible. The results and discussion in this paper are useful for researchers in the field of natural fiber-reinforced thermoplastic composite science, to help evaluate the mechanical properties of the interphase region.

Acknowledgements

The project was supported by the National Research Initiative of the USDA Cooperative State Research, Education and Extension Service, Grant number # 05-02645, Tennessee Agricultural Experiment Station, Project # 83. Instrumentation for the nanoindentation work was provided through the SHaRE Program at the Oak Ridge National Laboratory, which was sponsored by the Division of Materials Science and Engineering, U.S. Department of Energy under contract DE-AC05-000R22725 with UT-Battelle, LLC.

References

- [1] Keller A. Compounding and mechanical properties of biodegradable hemp fiber composites. *Compos Sci Technol* 2003;63(9):1307–16.
- [2] Mohanty AK, Misra M, Drzal LT. Surface modifications of natural fibers and performance of the resulting biocomposites: An overview. *Compos Interface* 2001;8(5):313–43.
- [3] Shibata M, Oyamada S, Kobayashi S, Yaginuma D. Mechanical properties and biodegradability of green composites based on biodegradable polyesters and lyocell fabric. *J Appl Polym Sci* 2004;92:3857–63.
- [4] Zini E, Baiardo M, Armelao L, Scandola M. Biodegradable polyesters reinforced with surface-modified vegetable fibers. *Macromol Biosci* 2004;4:286–95.
- [5] Oksman K, Skrifvars M, Selin JF. Natural fibres as reinforcement in polylactic acid (PLA) composites. *Compos Sci Technol* 2003;63(9):1317–24.
- [6] Nishino T, Hirao K, Kotera M, Nakamae K, Inagaki H. Kenaf reinforced biodegradable composite. *Compos Sci Technol* 2003;63(9):1281–6.
- [7] Lee SH, Wang S. Biodegradable polymers/bamboo fiber biocomposite with bio-based coupling agent. *Compos A: Appl Sci Manuf* 2006;37(1):80–91.
- [8] Lee SH, Ohkita T, Kitagawa K. Eco-composites from poly (lactic acid) and bamboo fiber. *Holzforschung* 2004;58(5):529–36.
- [9] Lee SH, Ohkita T. Bamboo fiber (BF)-filled poly (butylenes succinate) green-composite -Effect of BF-e-MA on the properties and crystallization kinetics. *Holzforschung* 2004;58(5):537–43.
- [10] Lee SH, Ohkita T. Mechanical and thermal flow properties of wood fiber-biodegradable polymers composites. *J Appl Poly Sci* 2003;90:1900–5.
- [11] Clemson C. Wood-plastics in the United States. *Forest Prod J* 2002;52(6):10–8.
- [12] Drzal LT. The interphase in epoxy composites. *Adv Polym Sci* 1986;75:1–32.
- [13] Kim JK, Mai YW. Engineered interfaces in fiber reinforced composites. New York, 1998: Elsevier; 1998.
- [14] Kim JK, Mai YW. Interfaces in composites. In: Chou TW, editor. *Materials science and technology: structure and properties of composites*, 13. Weinheim, Germany: VCH; 1993. p. 229–89 (chapter 6).
- [15] Drzal LT. In: Dusek K, editor. *Epoxy resins and composites II*. Springer-Verlag; 1986. p. 3–32.
- [16] Williams JG, Donnellan ME, James MR, Morris WL. Properties of the interphase in organic matrix composites. *Mater Sci Eng A* 1990;126:305.
- [17] Piggott MR. Tailored interphases in fiber reinforced polymers. *Mater Res Soc Symp* 1990;170:265.
- [18] Graham JF, McCague C, Warren OL, Norton PR. Spatially resolved nanomechanical properties of Kevlar® fibers. *Polymer* 2000;41:4761.
- [19] VanLandingham MR, Villarrubia JS, Guthrie WF, Meyers GF. Nanoindentation of polymers, an overview, advances in scanning probe microscopy of polymers. *Macromol Symp* 2001;167:15–43.
- [20] Downing TD, Kumar R, Cross WM, Kjerengtroen L, Kellar JJ. Determining the interphase thickness and properties in polymer matrix composites using phase imaging atomic force microscopy and nanoindentation. *J Adhes Sci Technol* 2000;14(14):1801–12.
- [21] Gao SL, Mäder E. Characterisation of interphase nanoscale property variations in glass fiber reinforced polypropylene and epoxy resin composites. *Composites: Part A* 2002;33:559–76.
- [22] Hodzic A, Stachurskia ZH, Kim JK. Nano-indentation of polymer–glass interfaces part I experimental and mechanical analysis. *Polymer* 2000;41:6895–905.
- [23] Li X, Bhushan B. A review of nanoindentation continuous stiffness measurement technique and its applications. *Mater Charact* 2002;48:11–36.
- [24] Munz M, Sturm H, Schulz E, Hinrichsen G. The scanning force microscope as a tool for the detection of local mechanical properties within the interphase of fiber reinforced polymers. *Composites: Part A* 1998;29A:1251–9.
- [25] Oliver WC, Pharr GM. An improved technique for determining hardness and elastic modulus using load and displacement sensing indentation experiments. *J Mater Res* 1992;7(6):1564–83.
- [26] Tze WTY, Wang S, Rials TG, Pharr G. Nanoindentation of wood cell wall: Continuous stiffness and hardness measurements, *Composite A*; Applied Science and Manufacturing, in review.
- [27] Gindl W, Konnerth J, Schoberl T. Nanoindentation of regenerated cellulose fibers. *Cellulose* 2006;13:1–7.
- [28] Bourban C, Karamuk E, deFondaumiére MJ, Ruffieux K, Mayer J, Wintermantel E. Processing and characterization of a new biodegradable composite made of a PHB/V matrix and regenerated cellulosic fibers. *J Environ Polym Degr* 1997;5(3):159–66.
- [29] Houshyar S, Shanks RA, Hodzic A. The effect of fiber concentration on mechanical and thermal properties of fiber-reinforced polypropylene composites. *J Appl Poly Sci* 2005;96:2260–72.
- [30] Kim JK, Sham ML, Wu JS. Nanoscale characterisation of interphase in silane treated glass fibre composites. *Compos Part A: Appl Sci Manuf* 2001;132(5):607–18.